

How auto- and cross-correlations in link dynamics influence diffusion in non-Markovian temporal networks

Oliver E. Williams,^{1,*} Fabrizio Lillo,² and Vito Latora^{1,†}

¹*School of Mathematical Sciences, Queen Mary University of London, London, E1 4NS, United Kingdom*

²*Department of Mathematics, University of Bologna, Piazza di Porta San Donato 5, 40126, Bologna, Italy*

(Dated: September 19, 2019)

Many real-world biological, social and man-made networks are inherently dynamic, with their links switching on and off over time. In particular, the evolution of these networks is often observed to be non-Markovian, and the dynamics of their links are often correlated. Hence, to accurately model these networks, the inclusion of both memory and dynamical dependencies between links is key. This being said, the interplay between memory and correlations in the dynamics of links, and its effects on processes taking place on the network, is not well understood. In light of this, we here introduce a simple generative model for temporal networks with a specified underlying structural backbone, and with precise control over the dynamical dependencies between links and the strength and length of their memories. In our model the presence of each link is influenced not only by its past activity, but also by the past activities of other links, as specified by a coupling matrix, which directly controls the interactions, and hence the correlations, among links. The model allows us to study the effects of both the memory parameter and correlations between links on the speed of a diffusion process over the network, as measured by the time taken for it to reach equilibrium. Further to this, we can effectively separate the roles of autocorrelations and neighbourhood correlations in link dynamics, allowing us to show, through both numerical simulations and analytical results, that not only is the speed of diffusion non-monotonically dependent on the memory length, but also that correlations among neighbouring links help to speed up the spreading process, while autocorrelations slow it back down. Our results have implications in the study of opinion formation, the modelling of social networks and the spreading of epidemics through mobile populations.

I. INTRODUCTION

Much of the world we experience is governed by interactions. Networks form an intuitive way of modelling these interactions, and as such the study of networks has been central to the understanding of both natural phenomena and man-made systems. Observably, many of these networks can be thought of as changing over time, as the connections and interactions that define them come and go; conversations and social interactions do not last forever [1–4], roads between towns and cities can be closed or new ones build [5, 6], financial or economic agents trade each day with different counterparts [7], and even our brains undergo significant changes throughout our lives [8–11]. Real-world examples of temporal networks are often found to have a plethora of structural and temporal features, many of which play key roles in defining the dynamics of the systems for which they form the backbone [12–19]. Several models aim to replicate these features by having intuitively realistic underlying dynamics. For example, models of human social interaction often rely on an underlying random walk, or brownian motion [3, 20]. Other models take a slightly more abstract approach, introducing the notion of node "activity" to control the presence of links [21–23]. The adaptations and extensions of these models do directly specify the

presence of empirically observed features such as memory, by which we here mean a dependence on some finite number of past states. Indeed, memory has been seen to play a role in many real world networks [2, 9, 24, 25]. It can also be useful in the definition of flow based communities [26–28], the dynamics of social interactions [29], and the controllability of temporal networks [30]. However, the area of study in which memory has received the most attention is its relation to spreading processes [31, 32]. When considering the spreading of an infection over a network the memory of the links can have a considerable effect on the rate of spreading of the disease, and can even cause dramatic changes to the so called "epidemic threshold" [33–36]. In diffusive systems memory directly induces the slow-down, or speed-up, of the spread of what might be considered "information", or some "material" [28, 31, 37–40]. This has been studied in the context of "higher order networks", and is often understood to be a result of the correlated bursts, and the induced lasting interactions that the non-exponential inter event times which define memory necessitate [31, 41–45]. What has been done, however, does not form a full picture. The memory of the links that make up a network naturally means that these links have strong correlations with their own recent past. It is common in real networks to have pairs of different links which are correlated with each other. Indeed, it seems natural to assume that links in a temporal network will have memory of each others past, rather than simply their own. The connections between the rate at which information spreads across a network

* o.e.williams@qmul.ac.uk

† v.latora@qmul.ac.uk

and the memory of links are deep, as are the connections between memory and link correlations. However, the way in which inter link correlations and memory interact, and the effects this interaction has on spreading and other dynamical processes occurring over temporal networks is not well understood.

Here we investigate the effects of an underlying “backbone” network structure, and of memory length and inter link correlations on diffusion over the temporal network. As such, we have developed a model in which all of these can be precisely controlled. We then take this model, and a number of backbone topologies from real world systems, and present a number of analytical results concerning its behaviour and how it affects diffusion, along with numerical results to the same effect. We find that the average time taken for diffusion to reach equilibrium on these networks is non-monotonically dependent on the memory length, in accordance with recent findings regarding epidemic spreading [35]. This is then explained analytically for the limit of no cross correlations. We also find that this time to equilibrium is highly dependent on how links in the temporal network are correlated, with weaker autocorrelations among links in favour of stronger correlations between neighbouring links speeding up diffusion. This is a surprising compliment to many recent works: while autocorrelation in links slows down diffusion, as explained by the induced bustiness of the link processes, correlations between neighbours speeds it up [28, 31, 35, 37–39, 41, 46–48].

II. THE MODEL

We are here interested in the effects that memory in the underlying temporal network has on the rate at which information, or some other quantity spreads throughout a system whose interactions change over time. In order to study this in a systematic way, in this section we introduce a model, that we name the *Correlated Discrete Auto-Regressive Network* model of order p , or in short the CDARN(p) model. Such a model allows us to generate temporal networks with precisely controlled strength and length of the memory, while also introducing a key feature of real-world networks, namely correlations between the evolutions of links over time, as produced by dependencies between their dynamics. The model relies on the following input parameters. The first ingredient is the $N \times N$ adjacency matrix B describing the structure of the underlying network backbone of N nodes and L links, i.e. defining, which pairs of nodes can be connected by links and which pairs cannot. The average link density within the backbone is then controlled by the parameter $0 < y < 1$, while $0 \leq q \leq 1$ and $p = 1, 2, \dots$ are respectively the strength and length of the memory component of the dynamics of the temporal network. Finally another matrix, the $L \times L$ link coupling matrix C , allows to indicate the pairs of links whose dynamics are correlated. In the last part of this section we will discuss how to de-

fine appropriate indicators for measuring the effects of memory on a dynamical process over temporal networks of different size and nature, such as the rescaled average time for a diffusion process to reach equilibrium.

A. Diffusion on a temporal network

Diffusion is, in its original sense, the physical process by which atoms and molecules move from regions of high concentration to regions of low concentration. This process has been seen as an analogue to processes in several other areas, such as opinion formation [49], the motions and social interactions of people [50], and the movements of capital through a financial system [51], and as such is amongst the most common ways of describing spreading phenomena in these areas. Indeed, diffusion finds uses in many other areas, where it is used as a linear approximation to non-linear systems, such at the Kuramoto model [52].

Complex networks, often form the backbone of many real world systems, and so it is natural to study diffusion over them [53, 54]. In a diffusive process on a network the flow of information, or some material, over a link is proportional to the difference in its concentrations at the two nodes. The natural way to study diffusion on a network is in terms of the so called Laplacian matrix, which forms the network analogue of the Laplace operator, which governs continuous time, continuous space, diffusion. Suppose we have a static undirected network with N nodes and adjacency matrix $A = \{a^{ij}\}$. The equation that governs the diffusion of some node related quantity $\underline{d}(t) \in \mathbb{R}^N$ over time can be written as:

$$\dot{\underline{d}}(t) = -\mu \mathcal{L} \underline{d}(t) \quad (1)$$

where μ is the diffusion coefficient, which controls the time scale of the diffusion process, and $\mathcal{L} = \{\mathcal{L}^{ij}\}$ is the graph Laplacian matrix, whose entries can be written in terms of the entries of A as $\mathcal{L}^{ij} = \delta(i, j)k_i - a^{ij}$, where $k_i = \sum_j a^{ij}$ is the degree of node i [54]. Notice that this equation is in continuous time; as a convention when a variable is continuously dependent on time, the time will be in brackets (e.g. $A(t)$), and for discrete time it will be given as an index (e.g. A_t). On a temporal network the only thing that needs to be changed in this equation is that the Laplacian matrix must be allowed to vary over time, hence $\mathcal{L} \mapsto \mathcal{L}(t)$ where $\mathcal{L}(t)$ is the Laplacian matrix associated to the continuous time adjacency matrix $A(t)$. This system exists in continuous time, and so the temporal network that underlies it must also exist in continuous time. The solution of the above equation is then clearly

$$\underline{d}(T) = \exp\left(-\mu \int_0^T \mathcal{L}(t) dt\right) \underline{d}(0)$$

However, the vast majority of models for temporal networks are discrete in time, and so, given a model for a discrete time temporal network, we must first embed the

network in continuous time. To this end, we assume that the adjacency matrix changes at discrete time steps of length Δt , taken, without loss of generality, to be equal to 1. Thus the Laplacian $\mathcal{L}(t)$ is piecewise constant and, according to the above notation, will be denoted by \mathcal{L}_t ($t = 1, \dots, T$). The solution of the diffusion equation hence becomes

$$\underline{d}_T = \exp\left(-\mu \sum_{t=1}^T \mathcal{L}_t\right) \underline{d}_0. \quad (2)$$

B. The CDARN(p) model

Models for temporal networks in which links are governed by a possibly correlated set of stochastic processes allow for a great deal of control over various aspects of their output, but can run the risk of being too abstract, and thus their use in describing empirical systems can be limited. For example, temporal networks in which links are specified to have an inter-event time with a Weibull distribution have been seen to reflect empirical findings with respect to infection spreading, and clearly imply memory in the network, however it is not clear that they are a good model for temporal networks in more general settings [55]. We here take the DARN(p) model, the simplest possible generalization of Erdős-Rényi random graph models to the case of temporal networks with memory [7, 35], and refine it so that it better reflects the presence of two key features of real systems [4, 8, 9, 38, 56]:

1. the existence of an underlying restriction, a so-called network “backbone” on which links can occur.
2. the presence of cross-correlations in link dynamics, i.e. of dynamical dependencies in the temporal activities of different links.

The DARN(p) model, originally introduced in [35] (See also [7]), generates a temporal network with precisely controlled memory features in the temporal sequence of each link. Namely, the model considers N nodes and assigns to each of the $N(N-1)/2$ pairs of nodes the presence or absence of a link as ruled by independent, identical DAR(p) processes (Discrete Auto-Regressive processes of order p) [7, 57–59]. In this way each link will, at each time step, either be generated randomly with some fixed probability, or will copy a randomly chosen state from its past p iterations. In terms of random variables, this would give us a temporal adjacency matrix $A_t = \{a_t^{ij}\}$, with $t = 1, 2, \dots$, where each link (i, j) , with $i, j = 1, \dots, N$ is governed by the process:

$$a_t^{ij} = Q_t^{ij} a_{(t-Z_t^{ij})}^{ij} + (1 - Q_t^{ij}) Y_t^{ij}. \quad (3)$$

where, for each link (i, j) and time t , Q_t^{ij} , Y_t^{ij} and Z_t^{ij} are random variables. In particular, $Q_t^{ij} \sim \text{Bernoulli}(q)$, $Y_t^{ij} \sim \text{Bernoulli}(y)$, and Z_t^{ij} is some random variable

which picks integers in the range $(1, \dots, p)$. Note that with this choice each link has the same unconditional probability of being present. We here take $Z_t^{ij} \sim \text{Uniform}(1, p)$. The networks created by the DARN(p) model are undirected, and clearly non-Markovian, with precise memory p .

The DARN(p) model assumes that links can occur between any two nodes. This is not always the case in real world networks, where certain links may be unfeasible, or simply impossible. For example, a plane may not be allowed to fly between two particular airports, or a doctor may be responsible for a small number of patients, and therefore not interact with others. We therefore say that these temporal networks have a “backbone”: a fixed set of possible links which restrict the networks evolution. With this in mind we make our first modification in a more general framework. First, we define a *backbone network* with L links described by a static $N \times N$ adjacency matrix $B = \{b^{ij}\}$. Then a temporal network on this backbone is represented by a $N \times N$ time-varying adjacency matrix $A_t = \{a_t^{ij}\}$, so that $a_t^{ij} = 0$ for all t if $b^{ij} = 0$, while if $b^{ij} = 1$ then the link (i, j) can exist for any value of t . In this way the presence of links can be appropriately limited to reflect reality.

Since links in the DARN(p) model are generated by independent processes, there can be auto-correlations in the temporal activity of each link, but no cross-correlations between different links. Conversely, correlations among different links are a natural feature of many systems. To further our earlier analogy, an airline is unlikely to schedule two flights between the same airports in close proximity to each other, but may prefer to schedule flights at appropriate times to make connections. Similarly doctors may see patients in a particular order each day, even if the duration of each interaction is not so consistent. In order to allow for such correlations, we introduce our second modification: when a link in a DARN(p) model would pick from its own memory, we now allow it to pick a link from the network at random, possibly itself again, and copy a randomly chosen state of that link instead. In this way, the dynamics of each link (i, j) that belongs to the network backbone is governed by the process:

$$a_t^{ij} = Q_t^{ij} a_{(t-Z_t^{ij})}^{M_t^{ij}} + (1 - Q_t^{ij}) Y_t^{ij} \quad (4)$$

with $i, j = 1, \dots, N$ and such that $b^{ij} = 1$, and where at each time t , M_t^{ij} is a random variable which associates to link (i, j) another link (i', j') among links which are present in the backbone B , with an assigned probability distribution. However, note that for each time t and link (i, j) , M_t^{ij} is independent and identically distributed. That is to say, if a link is to copy from the past of another link, then which link it chooses is completely independent on either the time, or the existence of any other link. If we label links with a linear index $(i, j) \mapsto \ell$, $(i', j') \mapsto \ell'$, with $\ell, \ell' = 1, 2, \dots, L$, then M_t can be characterised by

the probabilities:

$$\text{Prob}(\ell \text{ draws from } \ell') = c^{\ell\ell'}$$

These probabilities define a $L \times L$ row-stochastic matrix $C = \{c^{\ell\ell'}\}$, which we call the *coupling matrix*. By tuning the entries of this matrix we can specify the dependencies among links existing in our temporal network. In practice, for each possible link (i, j) and at each time t , M_t^{ij} will select another link (i', j') among a set of possible links associated to (i, j) , as given by matrix C . Then, the presence of the term $a_{(t-Z_t^{ij})}^{M_t^{ij}}$ in Eq. (4), represents the state of link (i', j') at one of the previous p temporal steps, and so will allow link (i, j) to copy its state at time t from one of the p past states of link (i', j') . The choice of the coupling matrix C is an important part of the CDARN(p) model, as this defines which links dynamics are correlated. Of course, there are many ways one could structure the matrix C , which we refer to as “coupling models”. Here, we will focus on the following three simple approaches: (i) only link autocorrelations but no cross correlations between different links, (ii) links are coupled to all other neighbouring links in the network backbone (as defined by B) with equal strength, (iii) links are coupled to all other links in the backbone with equal strength.

Together we then have our full model, which we name the *Correlated Discrete Auto-Regressive Network* model of order p , or in short CDARN(p) model. This model has the advantage of being able to introduce both auto- and cross-correlations in the link activities in a controlled way, allowing for a more realistic description of real world systems. It also retains a lot of the simplicity and tractability of the DARN(p) model. Indeed, two of the key features of the DARN(p) model that allow us to study a range of phenomena are exactly the same. Namely, the average degree of the network backbone is precisely that of an ER graph, $y(N-1)$ (See appendix A) [60]. Moreover, in the limit of long memory, as given by large p , the model is identical to a sequence of uncorrelated ER graphs (see appendix B). In summary, our model generates temporal networks $A_t, t = 1, 2, \dots$, with precisely controlled coupling among links, given the following set of control parameters: network backbone as specified by matrix B , link density y , memory strength q , memory length p , and link coupling matrix C . For our purposes we will assume that the links in the temporal network are undirected, we do this by identifying $a_t^{ij} = a_t^{ji}$. Implicitly the backbone in any network will be taken as undirected, implying that only symmetric matrices B will be considered. Finally, an important assumption of the CDARN(p) model is that the parameter p , q , and y are the same for all the links of the backbone. Of course this choice is a simplification only motivated by the need for control over the dynamics with a small number of parameters. The CDARN(p) model can in fact be easily generalized to the case of different parameters for each links, as done for instance in the simpler DARN(1)

model presented in [7].

C. Measuring the effect of memory on diffusion

As stated, our purpose here is to study the effects that memory in a temporal network has on diffusion over that network. This is a very general aim, and so we must be more specific about what we wish to analyse. Rather than studying spreading in terms of the full dynamics of diffusion on a temporal network, i.e. the concentrations \underline{d}_t of material at each node at each time step t , we can instead ask about how long it takes for this diffusion to reach equilibrium. In particular, since the changes in the network are responsible for any changes in the rate of spreading, we focus on the number of network evolutions (number of time steps Δt) before equilibrium. To formalise this concept we first note that in general we will not reach equilibrium in a finite number of timesteps, and so we instead fix some small positive ϵ , so that the *time to equilibrium* is then defined as:

$$\tau = \min_{t \in \mathbb{N}} (t : |\underline{d}(t) - \underline{u}| < \epsilon), \quad (5)$$

where the vector \underline{u} is the uniform vector with $u^i = 1/N$, which corresponds to the equilibrium state of the diffusion process on a connected network with N nodes. For our purposes the norm $|\cdot|$ will be taken to be the Euclidian norm. The temporal networks we will use here are generated by discrete-time random processes, and so τ will be a random variable. Given this, we will focus on finding the average of this value, $\langle \tau \rangle$, over several realizations of the system. Unfortunately, $\langle \tau \rangle$ will be highly dependent on the structure or size of any temporal network being studied, and so it would be impossible to draw conclusions about the influence of any model parameters in these systems. Our goal here is to study the effects of memory on spreading rate, and so we must introduce some way of comparing the time to equilibrium as a function of this memory as given by different networks. To this end we normalise τ by expressing it in terms of the time taken for a diffusion to reach equilibrium on the same backbone, but with a memoryless temporal network. In other words, we define the *rescaled time to equilibrium*, \mathfrak{T}^p , given memory length p , in terms of $\langle \tau^p \rangle$, the average time to equilibrium given memory length p , as:

$$\mathfrak{T}^p = \frac{\langle \tau^p \rangle}{\langle \tau^0 \rangle}. \quad (6)$$

Notice that the CDARN(p) model does not directly allow for $p = 0$, and so we define τ^0 to be the case where $q = 0$, and so no memory is ever used. This allows us to compare the effects that changing the memory length p and the coupling matrix C have on different backbones.

Backbone	N	$\langle k \rangle$	D	λ_N	λ_2
Airport	143	2.030	0.0143	31.02	0.01696
Email	167	38.93	0.2345	140.0	0.3811
Tube	302	2.311	0.0078	8.432	0.005918

TABLE I. **Key structural features for each backbone.** The number of nodes (N), average degree ($\langle k \rangle$), density (D), and dominant (λ_N) and smallest non-zero (spectral gap, λ_2) eigenvalues of the Laplacian matrix for each backbone.

III. NUMERICAL RESULTS

We have first investigated the rescaled time to equilibrium of a diffusion process on CDARN(p) temporal network models with different backbones by means of an extensive set of numerical simulations. The value of the parameter μ allows to tune the time scale of the diffusion process, while the three parameters controlling the link density y , memory strength q , memory length p , and the two matrices network backbone B , and link coupling matrix C , control the properties of the temporal network. To construct the backbones B we have taken three real-world temporal networks, each with different structural properties, and we have aggregated their links over the extent of the available network data and discarded the link weights. The three real temporal networks we have considered are: (i) Flights between US airports (Airport) [61]. (ii) Email interactions between employees at a manufacturing company (Email) [62]. (iii) Journeys on the London underground (Tube) [63]. The key features of the three resulting backbones are summarised in Table I. The number of nodes in the three networks ranges from about 100 to 300. With 302 nodes and an average degree $\langle k \rangle = 2.3$ the Tube is the backbone with the smallest link density, while Email is a very dense backbone with links connecting 23% of the possible pairs of nodes. Our aim here is to study not only the effects of memory, but also the interplay between memory and correlations in the dynamics of links. In order for us to clearly observe the effects of these features we must be able to compare different models: one in which the evolution of links is correlated, and one in which links are independent. As such we have simulated our system on each of the three different backbones B for a range of different parameters p, q, y and μ , and, for three different forms of the coupling matrix C . Specifically, the first case we have considered is the extreme one, in which there are no cross correlations at all between the evolution of links, so that each link is only correlated with itself. The second case we have considered is that of local cross correlations, where only links which share a node in the backbone B are correlated. The third case is that of uniform cross correlations, where all links in the backbone are correlated regardless of whether they are neighbours or not. To summarise, given a backbone B with L links, we have the three following coupling models:

1. The *no cross correlation (NCC)* coupling model,

where the coupling matrix reads $C = Id$ (the identity matrix).

2. The *local cross correlation (LCC)* coupling model, where the entries of the coupling matrix can be written as: $c^{\ell\ell'} = (1 - c)\delta(\ell, \ell') + \chi(\ell' \in \partial_B \ell) c / |\partial_B \ell|$, for coupling strength c . Here, χ is the indicator function, $\delta(\ell, \ell') = 1$ if $\ell = \ell'$ and 0 otherwise, and $\partial_B \ell$ is the neighbourhood of link ℓ in backbone B , i.e for $\ell = (i, j)$ $\partial_B \ell = \{\ell' = (i', j') : b^{i'j'} = 1 \text{ and } i' \in \ell \text{ or } j' \in \ell\}$.
3. The *uniform cross correlation (UCC)* coupling model, where the entries of the coupling matrix can be written as $c^{\ell\ell'} = (1 - c)\delta(\ell, \ell') + (1 - \delta(\ell, \ell'))c/(L - 1)$, for coupling strength c .

Notice that the parameter $0 \leq c \leq 1$ in the second and third coupling model allows us to tune the contribution of the cross correlations with respect to that of the auto-correlations. In particular the NCC model is the special case of the LCC and UCC models with coupling strength $c = 0$.

In our simulations, for each instance of diffusion on a CDARN(p) model, i.e. for each different set of parameters μ , and p, q, y, B, C and c , we extract the value of \mathfrak{T}^p . This is done directly by estimating $\langle \tau^p \rangle$ and $\langle \tau^0 \rangle$, where the averages are taken from multiple realisations of the diffusion process. In each case the initial condition for the diffusion \underline{d}_0 is such that all of the material to be diffused is placed at a random node j : $d_0^i = \delta(i, j)$ where $j \in \{1, \dots, N\}$. In this way we avoid any bias that might be introduced by repeatedly choosing the same starting node. Before any diffusion takes place on the temporal network, we allow the CDARN(p) temporal model to evolve until it has reached a steady state.

In Fig. 1 we report the rescaled time to equilibrium \mathfrak{T}^p given memory length p as a function of p , for each backbone and with a number of different sets of model parameters. Note that a semi-log scale has been used. To ensure that memory plays a significant part in the evolution of the temporal network we have fixed the memory strength $q = 0.95$, and to ensure that the system has enough time for the effects of memory to be observable we have fixed the link density $y = 0.1$. We then vary the diffusion speed $\mu = 0.1, 0.5$. All of these results are shown for both the local cross correlation model, with the three values of the coupling strength $c = 0.5, 0.3, 0.1$, and the no cross correlation model, i.e. the case $c = 0$. For $\mu = 0.1$, and hence slow diffusion, we observe that the equilibrium time is non-monotonically dependent on the memory length for all backbones, coupling strengths, and for both coupling models. This non-monotonicity is most prominent when $c = 0.1$, but far less so when the coupling is stronger. When we consider $\mu = 0.5$, and so faster diffusion, the observed non-monotonicity is far less apparent in all but the NCC model, there is however still a strong dependence on memory, particularly for lower values of c . Unsurprisingly, there is a significant difference between the results for the no correlation

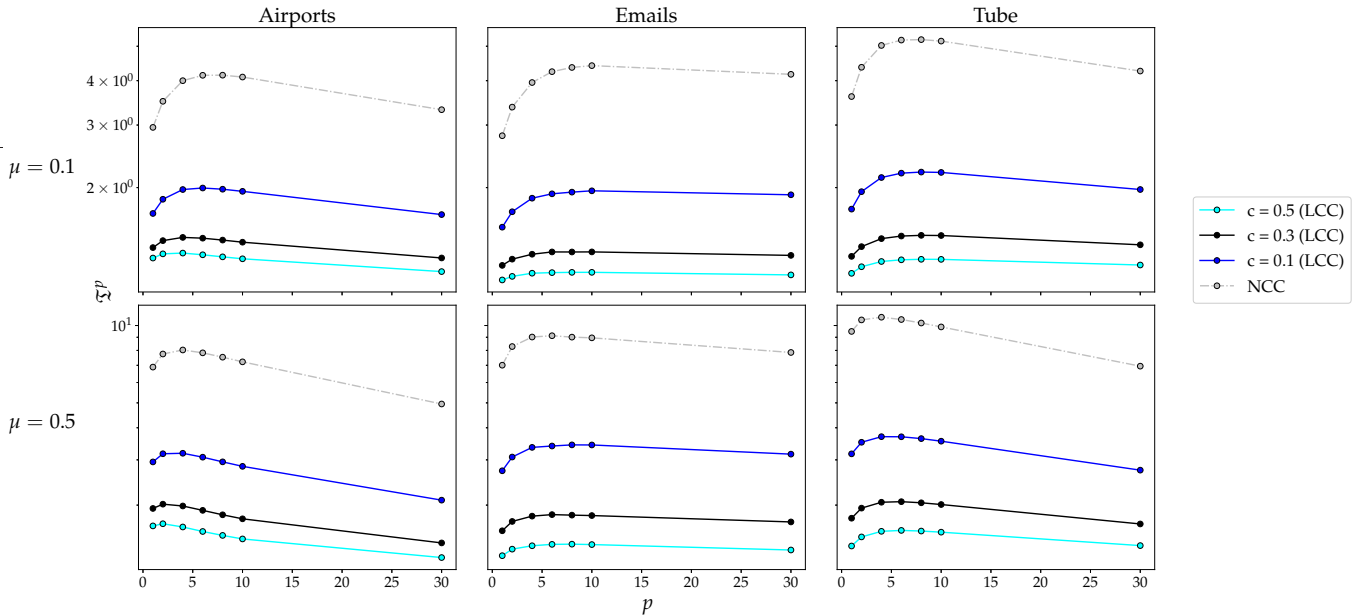


FIG. 1. **Rescaled time to equilibrium for diffusion on different network backbones as a function of the memory length p** for a CDARN(p) model with local (solid lines, LCC), and no (grey line, NCC) cross correlations between different links. Memory strength q is kept constant at 0.95 to ensure that memory plays a significant role in the evolution of the network and link density y is kept at 0.1 to ensure that there is sufficient time for any effects of memory to be observed. The coupling strength c and diffusion speed μ are varied. The backbones were taken from a collection of real data sets. Averages were taken over $2 \cdot 10^4$ realizations of the process. Note that a semi-log scale has been used.

model and those with correlations: in all cases local correlations speed up diffusion. What we do notice though is that there is no marked difference between different backbones. Since we have normalised each set of results this is not entirely unexpected.

In summary, the rescaled equilibrium time shows a number of interesting features as a function of the memory length p , the coupling matrix C and the backbone B . Most notable among these features are :

- The rescaled time to equilibrium \mathcal{T}^p is generally a non-monotonic function of the memory length p .
- Stronger local correlations, i.e. larger values of the coupling strength c speed up diffusion.
- Correlations have a considerable effect on the influence of memory: when the coupling strength c is high then diffusion properties are weakly dependent on the memory properties of the network.

As we will show in the following, by understanding the behaviour in the limit of no cross correlations, and by isolating the effects of temporal correlations, we can get a clear picture of the causes of our observations.

IV. THEORETICAL RESULTS

In light of our numerical results, we now study the theory which underpins both the CDARN(p) model and the diffusion of material over it. We will first study spreading in the limit of no cross correlations, that is when we adopt the NCC coupling model. We will then present a general analytical approach to finding the lagged cross and autocorrelations for an arbitrary coupling matrix C , which we will use in Section V to explore the interplay between correlations and memory in more depth than would be possible through simulations alone. In particular, we will use it to isolate the effects that correlations among neighbouring links in the LCC coupling model have on the time taken for diffusion processes on the temporal network to reach equilibrium.

A. Solution in the no cross correlations limit

We first study diffusion on the simplest form of the CDARN(p) model, the limit of no cross correlation between the dynamics of links. This is precisely the NCC coupling model that was previously introduced. In such a limit the links of the CDARN(p) model are independent processes, and so we can study them in isolation. In this case, as we will show below, the model is analyt-

ically tractable and it is possible to derive an analytical expression for the rescaled time to equilibrium.

In order to analyse the dynamics of diffusion over a single link of the CDARN(p) model, let us consider two nodes, one of which has an amount of a material, and the other of which has some other amount. The diffusion of this material out of the first node is given by:

$$\underline{\dot{d}}^1(t) = -\mu (d^1(t) - d^2(t)) a_t^{1,2}. \quad (7)$$

where the random variable $a_t^{1,2}$ describes the presence of the link between node 1 and node 2, and is governed by Eq. 3, the equation governing a DAR(p) process. When combined with the conservation condition $d^2(t) = 1 - d^1(t)$ this describes the full dynamics of the diffusion process. Given any set of initial conditions we can first find the number τ of time steps before equilibrium is reached. By noticing that, since when the link is not present there can be no diffusion, we only need to count the number of times that the link is present. If we were to take $a_t^{1,2} = 1$ for all t , then we can easily find $\tau = n$, and express n in terms of $\mu, \Delta t$ and ϵ (see appendix C). Now let us associate with $a_t^{1,2}$ the counting process $C_a(t) = \sum_{k=0}^t a_k^{1,2}$. We can then see that for a link that changes in time $\tau = \min_{t>0}(t : C_a(t) = n)$. This allows us to re-phrase our problem: we now want to find the average time taken until a link governed by a DAR(p) process has occurred n times. The DAR(p) process that governs the link can be thought of as a p -th order Markov process with the following transition matrix (see appendix D for a full explanation and discussion):

$$T_{\alpha\beta} = \left[q \frac{h(\alpha)}{p} + (1-q)y \right] \delta \left(\beta, 2^{p-1} + \lfloor \frac{\alpha}{2} \rfloor \right) + \left[1 - q \frac{h(\alpha)}{p} - (1-q)y \right] \delta \left(\beta, \lfloor \frac{\alpha}{2} \rfloor \right) \quad (8)$$

Here α and β represent some indexing of the $S = 2^p$ possible memory states, $h(x)$ is the Hamming weight of the number x (the number of 1's in its binary representation), $\delta(x, y) = 1$ if $x = y$ and 0 otherwise, and $\lfloor x \rfloor$ is the largest integer value smaller than x . If we break this matrix up into two parts, $T^L = \left[1 - q \frac{h(\alpha)}{p} - (1-q)y \right] \delta \left(\beta, \lfloor \frac{\alpha}{2} \rfloor \right)$ and $T^R = T - T^L$, then we can find the average time $k_\alpha \in \mathbb{R}_{\geq 1}^S$ taken for a link to occur given that it started in state α as [64, 65]

$$\underline{k} = (Id - \underline{T}^L)^{-1} \underline{\mathbf{1}}, \quad (9)$$

and the probability $h_{\alpha\beta}$ that when a link occurs it will occur in state β , given that it started in state α as

$$\underline{h} = (Id - \underline{T}^L)^{-1} \underline{T}^R. \quad (10)$$

Now let us define ω_α as the probability that a link starts in state α . We can then find the average time taken until the n -th link in a p -th order system as:

$$\langle \tau^p \rangle = \underline{\omega}^T \left(\sum_{t=0}^{n-1} \underline{h}^t \right) \underline{k}. \quad (11)$$

We now have an explicit formula for the average number of time steps to equilibrium. However, it is impossible to compare values of $\langle \tau^p \rangle$ directly, as such values will be heavily dependant on parameters of the model other than the memory length p , regardless of the interaction between those parameters and the memory. Because of this, we look at the rescaled time to equilibrium as defined in Eq. 6. The limiting behaviour of this quantity can be studied analytically. First, we note that $\langle \tau^0 \rangle$ can be found directly as n/y . Then, we observe that as $p \rightarrow \infty$, $\langle \tau^p \rangle \rightarrow n/y$ (see appendix B and E), meaning that our large memory limit is exactly the same as the no memory case, and because of this \mathfrak{T}^p is not intrinsically bounded above (see appendix E). We can also directly solve for $p = 1$, and in principle extend these calculations to solve for small p (see appendix E). Finally we can show that, when y is ‘‘small enough’’, as it is in all of our cases, $\langle \tau^p \rangle \geq \langle \tau^\infty \rangle$, and hence that

$$\mathfrak{T}^p \geq 1. \quad (12)$$

Hence the rescaled equilibrium time in the large memory limit acts as a lower bound for the case of arbitrary p (see appendix F), explaining the similar behaviour observed in the full system. It should be noted that in cases where y is not ‘‘small enough’’ we will observe the opposite effect: the large memory limit will be an upper bound.

When plotting this rescaled time to equilibrium as a function of p for various μ and y , as in Fig. 2, we observe many of the same traits we found in Section III for the full CDARN(p) model with cross correlations. Principally, the following two similarities need to be noted. Firstly we see evidence for the previously explained large memory limit, i.e. the rescaled time to equilibrium is bounded below by the value obtained in the limit of large p . Secondly we see that \mathfrak{T}^p can be highly non-monotonic as a function of p .

In summary, the study of the CDARN(p) model in the limit of no-cross correlations provides us with a good understanding of the causes for two of the most notable phenomena observed in the full network systems, and allows us to focus on the role of correlations in inducing the remaining effects.

B. Derivation of the temporal correlation matrix

The results of Section III clearly indicate that the presence of coupling in the temporal dynamics of different links plays an important role in the behaviour of the rescaled time to equilibrium for a diffusion process on a temporal network. Indeed our claim is that, while the temporal correlations of links with themselves slows down diffusion [28, 31, 37, 39, 41], as evidenced by the limit of no cross correlations case, temporal correlations among neighbouring links speeds it up. Fortunately, the CDARN(p) model is analytically tractable enough for us to fully describe the correlations that are present for a

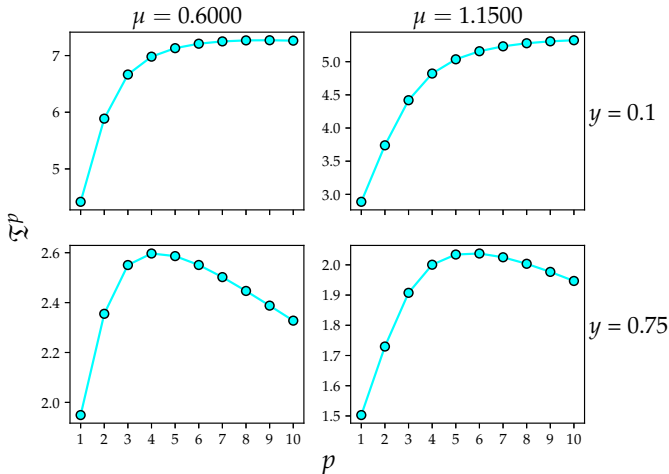


FIG. 2. **Rescaled time to equilibrium for diffusion over a link** in the limit of the CDARN(p) model with no cross correlations as a function of the memory length p . The dynamics of the link is generated by a DAR(p) model with $q = 0.95$, for various values of y . Two different values of diffusion constant μ were used.

general coupling matrix C , without relying wholly on simulations.

Rather than working with the backbone network directly, we will instead consider the corresponding graph in which links are the nodes in the backbone, and we connect any two nodes in the new graph if their links in the backbone graph shared a node. For a backbone network with L possible links, we assign each of these links with a linear index. Then let us denote the correlations between link ℓ and ℓ' at time lag k as $\langle A_t^\ell A_{t-k}^{\ell'} \rangle = \rho_k^{\ell\ell'}$. Given a coupling matrix C , $\rho_k^{\ell\ell'}$ can be found as the solution to the following Yule-Walker equations [57, 66]:

$$\rho_k = \frac{q}{p} C \sum_{a=1}^p \rho_{k-a}. \quad (13)$$

Note that we have dropped our indices, and so each element in the equation is a matrix. We can show that, for general C , this equation is solved by the composition of different functions over supports $k \in \{np, \dots, (n+1)p\}$ for integer n . The first of these can be found to be constant, while the following are exponentially decaying (see appendix G, H). Because of this, we can characterise the correlations at all values of k in terms of this initial constant, which we call ρ . We first define the following tensor:

$$\Delta^{\ell\ell'\ell''} = \frac{q}{p} \left((p-1)c^{\ell\ell''} + q \sum_{b \neq \ell'} c^{\ell b} c^{b\ell''} \right), \quad (14)$$

then $\rho^{\ell\ell'}$ can be found as the solution to the following

system of linear equations (see appendix H)

$$\rho^{\ell\ell'} = \sum_{\ell''=1}^p \Delta^{\ell\ell'\ell''} \rho^{\ell''\ell'} + \frac{q}{p} c^{\ell\ell'}. \quad (15)$$

The system can be greatly simplified in special cases (see appendix H, I, J). For example, in the case of the UCC coupling model, we show that $\rho^{\ell\ell}$ is constant for all ℓ , and similarly $\rho^{\ell\ell'}$ is constant for all pairs ℓ, ℓ' such that $\ell \neq \ell'$, thus reducing the calculation of the correlation coefficients to solving a pair of linear simultaneous equations. Given this set of equations for $\rho^{\ell\ell'}$, we can also then find the correlations $\langle A_t^\ell A_t^{\ell'} \rangle = \rho_0^{\ell\ell'}$ when $\ell \neq \ell'$ as

$$\rho_0^{\ell\ell'} = q \sum_{\ell''=1}^L c^{\ell\ell''} \rho^{\ell''\ell'}. \quad (16)$$

This gives us a full picture of the correlations present in the CDARN(p) model and allows us to calculate them directly.

V. QUANTIFYING THE EFFECTS OF CORRELATIONS

We saw in our study of diffusion in the limit of no cross correlations that the rescaled time to equilibrium \mathfrak{T}^p is a non-monotonic function of the memory length p . It is also widely understood that a way of characterising memory of a time series is by using the autocorrelation function. We find for a CDARN(p) process the memory p is precisely the value for the time lag k after which the autocorrelation function ρ_k decays exponentially (see appendix G, and results in [35]). With this in mind we can now focus on the comparison between autocorrelation coefficients of links in a CDARN(p) temporal model and the cross correlation coefficients of neighbouring links. In order to do this effectively for large networks we will average these quantities over all links (and neighbours where appropriate) to gain the averaged autocorrelation coefficient ρ_{ac} and the averaged neighbourhood correlation coefficient ρ_{ncc} . These are defined, given the matrix of correlation coefficients $\rho^{\ell\ell'}$ for a backbone B with L links derived in Section IV B, as

$$\begin{aligned} \rho_{ac} &= \frac{1}{L} \sum_{\ell=1}^L \rho^{\ell\ell}, \\ \rho_{ncc} &= \frac{1}{L} \sum_{\ell=1}^L \frac{1}{|\partial_B \ell|} \sum_{\ell' \in \partial_B \ell} \rho^{\ell\ell'}. \end{aligned} \quad (17)$$

where as before $\partial_B \ell$ is the set of links in the neighbourhood of ℓ on the network backbone B .

For clarity, let us now re-state our claim, as based on our observations of the numerical simulations displayed

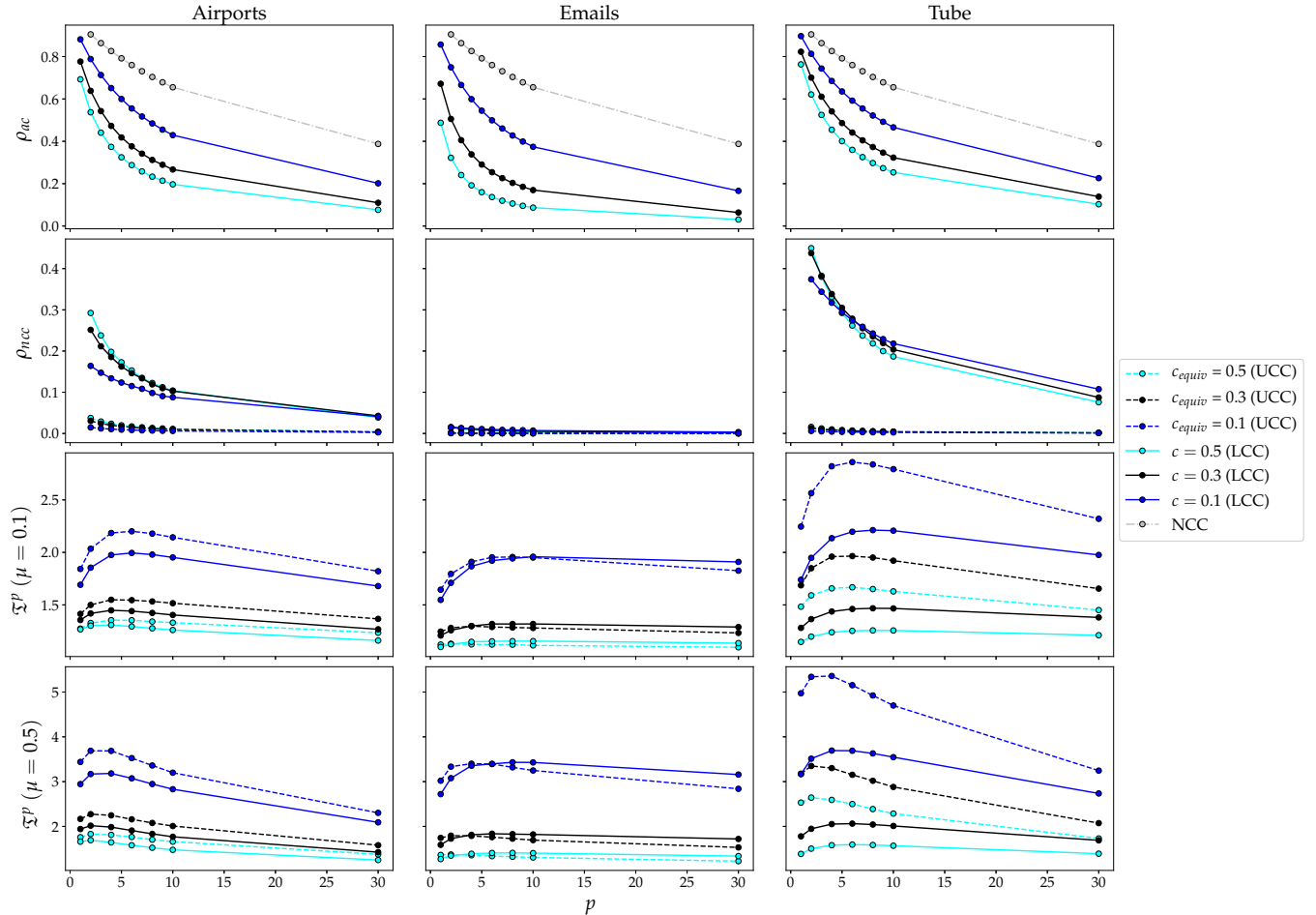


FIG. 3. **Average autocorrelation and neighbourhood correlation of a link, and rescaled time to equilibrium for diffusion** for both the LCC and UCC coupling models on different backbones as a function of the memory length p . The value of the average ρ_{ac} (first row), and ρ_{ncc} (second row), where averages are taken over links in a CDARN(p) temporal network with local cross correlation (solid line, LCC), uniform cross correlation (dashed line, UCC), and no cross correlation (dash/dot line, NCC) coupling, for each backbone. The third and fourth rows display the rescaled average time till equilibrium for a diffusion process on these networks with diffusion constants $\mu = 0.1$ and $\mu = 0.5$ respectively. Note that UCC is not included in the first row (ρ_{ac}) as its values are, by construction, precisely the same as those of the LCC model. The NCC model is not included in the second row (ρ_{ncc}) as its value is always zero. Memory strength q is kept constant at 0.95 to ensure that memory plays a significant role in the evolution of the network and link density y is kept at 0.1 to ensure that there is sufficient time for any effects of memory to be observed. The coupling strength c and diffusion speed μ are varied. Note that for the UCC model we assign the curves the value c_{equiv} rather than c , this is because we chose the values of c to match the value of ρ_{ac} for the UCC and LCC coupling models, as such c_{equiv} refers to the value of c in the LCC model that is being matched. The backbones were taken from a collection of real data sets. The rescaled times to equilibria were averaged over $2 \cdot 10^4$ realizations of the process.

in Fig. 1 : while autocorrelation of links slows down diffusion, correlations between neighbouring links speeds up diffusion. While in Fig. 1 we do see that diffusion is faster in the LCC model than in the NCC model, the autocorrelations of links in the two models are different. Further to this, while it would be possible to tune the parameters of the NCC model so that it produced links with the same autocorrelation coefficient as the LCC model, as the NCC model does not have a coupling strength, this

could only be achieved by changing either the memory strength q or the memory length p . Because of this we can not judge the influence of neighbourhood correlations from our previous results, and we cannot use the NCC model to explore the effects of neighbourhood correlations further. In order to give a valid point of comparison, we can now make use of our third coupling model, which allows us to precisely control the average link autocorrelation, but also removes any correlations between

neighbouring links. To recall, for a backbone with L links, the coupling matrix in the UCC model $C = c^{\ell\ell'}$ is given by $c^{\ell\ell'} = (1 - c)\delta(\ell, \ell') + (1 - \delta(\ell, \ell'))c/(L - 1)$. The simplicity of this model lends itself well to analytical calculations, and so we can now use this model to isolate the effects of neighbourhood correlations. Indeed we can show that in the limit of large numbers of links L this model reduces to a DARN(p) temporal network on a fixed backbone, in which links are independent (see appendix K). First we fix the parameters p, q and y for both the LCC and UCC models, this ensures that there is the same memory strength and length, and the average degree of the temporal networks produced are the same. We can then fix the value of c for the LCC model, as shown in Fig. 3 (first row), and calculate the resulting value of ρ_{ac} and ρ_{ncc} . By then varying the value of c used in the corresponding UCC model we obtain precisely the same value for ρ_{ac} , while leaving $\rho_{ncc} \approx 0$, because in the considered network backbones the number of links L is large. In figure 3 we plot both the values for ρ_{ac} and ρ_{ncc} , along with the rescaled time till equilibrium for a diffusion process on the corresponding temporal network. Note that the LCC and UCC models have, by construction, exactly the same value of ρ_{ac} , and so only LCC is plotted in the upper panels, and the NCC model must always have $\rho_{ncc} = 0$, and so it is not plotted in the lower panels.

We observe here that, as expected, the value of ρ_{ac} in the NCC model is significantly higher than for the LCC model. We also see that both ρ_{ac} and ρ_{ncc} decay as the memory length p increases, consistent with the DARN(p) temporal network model. Most notably, there are significant differences between the values of ρ_{ncc} given for each backbone. While both the Airport and Tube backbones display significant neighbourhood correlations in the LCC coupling model (though the values are larger for the Tube backbone), the Emails backbone only has notable neighbourhood correlations for low values of p , and indeed at $p = 30$ is practically indistinguishable from the NCC model. Also, as expected the value of ρ_{ncc} for the UCC model is always approximately 0. We have tested our hypothesis by comparing the rescaled time to equilibrium (see the lower two rows of Fig. 3) \mathfrak{T}^p for both the LCC and UCC models, both generated and plotted in exactly the same way as was done for Fig. 1. It is clear that when the value of ρ_{ncc} is large, as in the Tube backbone, diffusion on the LCC coupling model is always faster. When ρ_{ncc} is lower, as in the Airports backbone, this is still true. Finally, when there are little to no correlations between neighbours, as with the Email backbone, diffusion on the LCC coupling model is only faster than on the UCC model for small values of p , after this point the value of ρ_{ncc} is so small that its effects are no longer apparent. While the results for the Email backbone indicate that correlations among neighbours are not the only influence on behaviour, it is clear that their presence does act to speed up diffusion processes over the temporal network.

VI. CONCLUSIONS

The influence that memory in temporal networks has on process that run on them is increasingly seen as key to our understanding of the way that our highly networked world operates. In the context of spreading processes on temporal networks, such as the passage of infections or the diffusion of information, it has been observed that the presence of memory can either speed up or slow down the spreading relative to some memoryless case. This result has been observed here in a manner reminiscent of other recent findings. What is generally less well understood is precisely how memory causes this change in the speed of spreading. A great deal of work has gone into the studying of how the correlated bursts in link activity that are the result of non exponential inter link times, and hence memory, slow down spreading processes. This however does not yet give us a full picture.

Here we have presented a simple, flexible and controllable generative model for temporal networks which allows for arbitrary "backbone" topologies, and precise control over the memory strength, memory length, average degree, and coupling strength. Not only this, but the model is simple enough to allow an analytical treatment of a number of problems, including finding the exact correlations between any two links. Given this we have been able to study exactly how the memory and coupling in our model influence spreading processes on them. In doing this we have provided a solution to the time taken for a diffusion process in the limit of no cross correlations to reach equilibrium as a function of the memory length p . This shows us that the spreading time is non-monotonically dependent on p , and allows us to infer that the equivalent memoryless process provides the fastest possible diffusion in our model. Looking at networks we have shown that correlations play a more subtle role than might previously been expected. While we find, in accordance with previous works, that non-exponentially decaying autocorrelations among links do slow down diffusion, we, surprisingly, see that the opposite is true of local correlations. When links that share a node are correlated, this tends to speed up diffusion. This is made clear by the fact that when we observe a system in which links have fixed autocorrelation, but the correlations between neighbouring links varies (while all other parameters are kept constant), then diffusion is faster when correlations among neighbours are higher. This has strong implications for real world systems. While it is understood that memory and correlations between links has an effect on the spreading of information, the observation that correlations between neighbours and autocorrelations behave in opposite ways directly contributes to our understanding of many Empirical systems. For example, when considering the diffusion of information over a social network, and any consequent formation of opinions, correlations between social ties must be considered as important as the correlation of a social tie with its own history. In a more general sense our findings also

suggest that considering the evolution of links as independent processes in a temporal network means we lose a significant amount of information. Hence when assessing the properties of an empirical network correlations between the evolutions of links must be taken into account. Finally, we have been able to take the backbones used in testing from real world systems. This demonstrates the important role that such topologies play. It is clear that memory, correlations and backbone interact in a complex manner, and when considering the study of real world systems one can not assume to study of any of these features in isolation. Here, however, we have provided a framework in which the interplay between these features can be studied systematically, and how surprising results occur when we do.

ACKNOWLEDGMENTS

VL work was funded by the Leverhulme Trust Research Fellowship CREATE: the network components of creativity and success. We also thank Piero Mazzarisi and Lucas Lacasa for useful discussions.

AUTHOR CONTRIBUTIONS

All the authors designed the research. O.W. performed calculations and generated figures. All the authors discussed intermediate and final results and wrote the paper.

COMPETING INTERESTS

The authors declare no competing interests, financial or otherwise.

CORRESPONDANCE

Correspondence and requests for materials should be addressed to O.W or V.L.

VII. APPENDIX

A. Average degree of the CDARN(p) network

Our aim is to show that a CDARN(p) network on a complete backbone has the same average degree as a DARN(p) network, and hence as an ER random graph. To do this we need only show that the average value of an arbitrary link is given by $\langle a_t^{ij} \rangle = y$. Let us proceed by first averaging over the left and right hand sides of

Eq. 4 to get

$$\langle a_t^{ij} \rangle = q \langle a_{(t-Z_t^{ij})}^{M_t^{ij}} \rangle + (1-q)y. \quad (18)$$

If we now substitute the link i, j with its linear index ℓ we obtain the following:

$$\begin{aligned} \langle a_t^\ell \rangle &= \frac{q}{p} \sum_{s=1}^p \sum_{b=1}^L c^{\ell b} \langle a_{t-s}^b \rangle + (1-q)y, \\ &= q \sum_{b=1}^L c^{\ell b} \langle a_t^b \rangle + (1-q)y. \end{aligned} \quad (19)$$

In the above we have made use of the stationarity of this sequence to say that $\langle a_{t-a}^\ell \rangle = \langle a_t^\ell \rangle$. One can see also that $\langle a_t^\ell \rangle = \bar{a}$, for some constant \bar{a} , is a solution to the above equations. The fact that C is row stochastic, and so its rows sum to 1, then gives us that $\bar{a} = y$ is the unique solution. Hence we have maintained the average degree of the DARN(p) model.

B. The infinite memory limit

One of the key features of the DARN(p) model is that as $p \rightarrow \infty$ the temporal network becomes indistinguishable from a sequence of independent ER graphs. Our aim now is to show that this holds for the CDARN(p) model. We start by writing the conditional probability for a single link with linear index ℓ :

$$\text{Prob}(a_t^\ell = 1 | \{a_s\}_{s=t-1}^{t-p}) = (1-q)y + q\phi_t(p), \quad (20)$$

We hence see that our problem can be reduced to a study of the properties of some kernel function ϕ , defined as the probability that a 1 is drawn from any point in the memory, i.e.

$$\phi_t(p) = \sum_{\ell'} c^{\ell \ell'} \frac{1}{p} \sum_{k=1}^p a_{t-k}^{\ell'}. \quad (21)$$

We recognise the sample expectation over the past p steps of the time series, and so can see that $\phi_t(p) \rightarrow y$ as $p \rightarrow \infty$. For completeness we must also check that any fluctuations away from the mean can be ignored at finite times. First we see the following

$$\begin{aligned} \phi_{t+1}(p) - \phi_t(p) &= \sum_{\ell'} c^{\ell \ell'} \frac{1}{p} \sum_{k=1}^p (a_{t-k+1}^{\ell'} - a_{t-k}^{\ell'}), \\ &= \frac{1}{p} \sum_{\ell'} c^{\ell \ell'} (a_{t-k+1}^{\ell'} - a_{t-k}^{\ell'}). \end{aligned} \quad (22)$$

Once again we have that $a_{t-k+1}^{\ell'} - a_{t-k}^{\ell'} \in \{-1, 0, 1\}$, and so

$$-\frac{1}{p} \leq \phi_{t+1}(p) - \phi_t(p) \leq \frac{1}{p}, \quad (23)$$

$$\implies y - \frac{t}{p} \leq \phi_t(p) \leq y + \frac{t}{p}. \quad (24)$$

Hence, in the large p limit then the memory kernel ϕ tends to 0, and so the system is equivalent to one in which there is no memory. This displays exactly the same behaviour as is found for the DARN(p) model: the CDARN(p) model does indeed tend to a memoryless model in the limit of large memory. In the memoryless case we note that $\text{Prob}(a_t^\ell = 1) = y$, and so must have an expected inter-link time of $1/y$, and correspondingly the expected time until the n -th link is n/y .

C. Required number of links in the two node system

Consider the equations defining diffusion in continuous time between two nodes, for which the link between them is permanent:

$$\dot{d}^1(t) = -\mu(d^1(t) - d^2(t)). \quad (25)$$

If we impose conservation, i.e. $d^2(t) = 1 - d^1(t)$, (and drop the 1 so that $d^1(t) \rightarrow d(t)$) we can rewrite this as

$$\dot{d}(t) = \mu - 2\mu d(t). \quad (26)$$

This equation can be solved to find

$$d(t) = \frac{1}{2}(e^{-2\mu t} + 1). \quad (27)$$

We say that this system has reached equilibrium at the first time (in a continuous sense) $t = \tau_c$ where $|d^1(t) - d^2(t)| < \epsilon$ for some small positive ϵ . Again, imposing conservation this can be rewritten as the first value of t such that $2d(t) - 1 = \epsilon$. With Eq. 27 we can then find the (continuous) time to equilibrium directly as

$$\tau_c = \frac{-\log \epsilon}{2\mu}. \quad (28)$$

Hence the number of full time steps τ of length Δt which must occur before equilibrium is reached is given by

$$\tau = \lfloor \frac{-\log \epsilon}{2\mu \Delta t} \rfloor. \quad (29)$$

Note that for this system, for any given values of μ and Δt we can always find $\bar{\mu} = \mu \Delta t$, meaning that we may fix $\Delta t = 1$ and still recover the full range of possible dynamics.

D. The transition matrix for a DAR(p) variable

A full explanation of the transition matrix for a DAR(p) variable can be found in [35], however we will here provide enough detail for this work to be understood without further reading. Consider a DAR(p) random variable, as governed by the equation

$$X_t = Q_t X_{(t-Z_t)} + (1 - Q_t) Y_t, \quad (30)$$

where, for each t , $Q_t \sim \text{Bernoulli}(q)$, $Y_t \sim \text{Bernoulli}(y)$ and Z_t picks integers uniformly from the range $(1, \dots, p)$. This can be thought of as a p -th order Markov chain, and so is equivalent to a first order Markov chain in an enlarged state space [66]. Accordingly we define the so-called “ p -state” of link (i, j) at time t , by combining the state of the link at time t along with its previous $p - 1$ states in the vector $\underline{S}_t = (X_t, X_{t-1}, \dots, X_{t-p+1})$. If we now define the set \mathcal{S} as the set containing all 2^p possible p -states, then for any $\alpha, \beta \in \mathcal{S}$ we can look at the conditional probability $\text{Prob}(\underline{S}_{t+1} = \beta | \underline{S}_t = \alpha)$. This defines the entries of the p -th order $2^p \times 2^p$ transition matrix $T_{\alpha\beta}$.

E. Average time to equilibrium for a single Markov link

The value of the average time until a diffusion process across a single DAR(1) link, as denoted by $\langle \tau^1 \rangle$, is central to any analysis of the relevant rescaled time to equilibrium. Hence we calculate it explicitly here. We know that, given the value $\tau = n$ from Eq. 29 giving the number of time steps until equilibrium in a deterministic system, $\langle \tau^1 \rangle$ will be given by the equation

$$\langle \tau^1 \rangle = \underline{\omega}^T \left(\sum_{t=0}^{n-1} \underline{h}^t \right) \underline{k}. \quad (31)$$

Now \underline{h} will be a 2×2 matrix, and $\underline{\omega}$ and \underline{k} will be two dimensional vectors. To progress further we must now impose an ordering on the states $\alpha, \beta \in \mathcal{S}$. This is done by associating a linear index $l(\alpha)$ to each possible state $\alpha \in \mathcal{S}$ (and similarly for β). The simplest form of this labelling function, given that the memory length is p , which we will here use, is

$$l(\alpha) = \sum_{k=0}^{p-1} 2^k \alpha_k, \quad (32)$$

where α_k is the k th entry in the p -state vector associated with α . This is essentially taking the set of 0's and 1's that represent the link histories contained in α and converting them to a decimal number as if they were in binary. We will implicitly assume that wherever we use α , or any state in \mathcal{S} , we are referring to the label $l(\alpha)$. Given the definition of $h_{\alpha\beta}$ as the probability that a system starting in state α ends in state β , we can easily see that the following must be true:

$$\underline{h} = \begin{pmatrix} 0 & 1 \\ 0 & 1 \end{pmatrix}, \quad (33)$$

and so

$$\sum_{t=0}^{n-1} \underline{h}^t = \begin{pmatrix} 1 & n-1 \\ 0 & n \end{pmatrix}. \quad (34)$$

Similarly we may find that $\omega_1 = 1 - y$ and $\omega_2 = y$, and $k_1 = ((1 - q)y)^{-1}$ and $k_2 = y^{-1}$. Giving us the equation

$$\langle \tau^1 \rangle = \left(\frac{1}{1 - q} + n - 1 \right) \frac{1 - y}{y} + n. \quad (35)$$

It is then a simple matter to extend this result and calculate the value of \mathfrak{T}^1 directly. Given that we know $\langle \tau^p \rangle \rightarrow n/y$ as $p \rightarrow \infty$, and this is precisely the value of $\langle \tau^0 \rangle$, we then find

$$\frac{\langle \tau^1 \rangle}{\langle \tau^0 \rangle} = \left(\frac{1}{1 - q} + n - 1 \right) \frac{1 - y}{n} + y. \quad (36)$$

It is easy to see that the maxima and minima of this function in terms of n and y are finite and occur at their limiting values ($y = 0, 1$ and $n = 1, \infty$ respectively) if $q \neq 1$. However in the limit $q \rightarrow 1$ we see that $\mathfrak{T}^1 \rightarrow \infty$. In the $q = 0$ limit we obtain the value $\mathfrak{T}^\infty = 1$, as expected.

F. Rescaled time to equilibrium in the limit of large p

In the main text we claim that $\mathfrak{T}^p \geq 1$ for suitably sparse initial conditions, but that in other cases the opposite is true. To understand this we first equate our statement to saying that, given an initial probability vector $\underline{\omega}$, $\langle \tau^p \rangle \geq \langle \tau^\infty \rangle$, provided that the entries representing states in which no link is present (in our case ω_α for $\alpha \in \{1, \dots, 2^{p-1}\}$) contain the majority of the probability. Recall first that we are implicitly labelling our states $\alpha \in \mathcal{S}$ according to the labelling function given in Eq. 32. Now, notice that, since $\underline{\omega}$ is a probability vector, and \underline{h} is a stochastic matrix, we can define a vector \underline{k}^0 such that $k_\alpha^0 = 1/y$ for all α , and we can write the following equation:

$$\langle \tau^\infty \rangle = \underline{\omega}^T \left(\sum_{t=0}^{n-1} \underline{h}^t \right) \underline{k}^0. \quad (37)$$

Hence we can write

$$\langle \tau^p \rangle - \langle \tau^\infty \rangle = \underline{\omega}^T \left(\sum_{t=0}^{n-1} \underline{h}^t (\underline{k} - \underline{k}^0) \right). \quad (38)$$

By construction $h_{\alpha\beta} = 0$ if $\beta < 2^{p-1}$, and so if we define

$$\tilde{\underline{\omega}}^T = \underline{\omega}^T \left(\sum_{t=0}^{n-1} \underline{h}^t \right), \quad (39)$$

then when $\beta < 2^{p-1}$, $\tilde{\omega}_\beta = \omega_\beta$. Hence we see that if $\omega_0 \approx 1$ (the entry in ω representing an initial state with no links), then we need only check that $k_0 > 1/y$. To explore this further, first we write our definition of \underline{k} as the following set of linear equations:

$$k_\alpha = 1 + T_{\alpha\alpha'} k_{\alpha'}, \quad (40)$$

where $\alpha' = \lfloor \alpha/2 \rfloor$. From this we can directly obtain

$$k_0 = \frac{1 - qp^{-1}}{(1 - q)y}, \quad (41)$$

and hence confirm that $k_0 > 1/y$. We now want to understand the conditions in which this breaks down. One can manually check that, for and p , $k_\alpha > 1/y$ for $\alpha = 0, 1$, but that this inequality does not generally hold for $\alpha = 4$. As a specific example of this, if we fix $p = 3$, $y = 0.01$ and $q = 0.1$ then $1/y = 100$, but $k_4 \approx 98.52$. To understand this behaviour, we can then make use of the following two facts about k_α : given a memory state $\alpha \in \mathcal{S}$

- if α_n is the memory state with a 1 in the n -th entry, and zeros elsewhere, then the values of k_{α_n} are given by solutions to the equation $x_{n+1} = 1 + cx_n$, with appropriate values for c and x_1 .
- if β is the memory state obtained by taking memory state α and replacing any of its 0 states with 1, then $k_\beta < k_\alpha$.

To prove the first of these statements, we directly analyse Eq. 40. This equation, in our α notation becomes $k_{\alpha_{n+1}} = 1 + T_{\alpha_{n+1}, \alpha_n} k_{\alpha_n}$, but we also notice that $T_{\alpha_{n+1}, \alpha_n}$ is invariant on n , always taking the value $T_{\alpha_{n+1}, \alpha_n} = 1 - q/p - (1 - q)y$, which we will now denote as T . To obtain the desired form of difference equation, we now simply identify $x_n = k_{\alpha_n}$ and $c = T$. This can be easily solved to give the following:

$$k_{\alpha_n} = \frac{T^n}{(1 - q)y} + \frac{1 - T^n}{1 - T}. \quad (42)$$

This equation must clearly be decreasing with n .

To prove the second of these statements consider two possible memory states α and β , where β is given by taking α and replacing one of the zeros in its memory with a one. Let us label the position of the state which we change with t . Now let us now denote $\alpha^{(n)} = \lfloor \alpha^{(n-1)}/2 \rfloor$, where $\alpha^0 = \alpha$, and similarly for β . To clarify, we can think of $\alpha^{(n)}$ as being the memory state α shifted back n times, or similarly what happens to the memory state of a DAR(p) process if it starts in state α and generates n zeros. We can then write the following equation directly from Eq. 40:

$$k_{\alpha^{(n)}} - k_{\beta^{(n)}} = T_{\alpha^{(n)}\alpha^{(n+1)}} k_{\alpha^{(n+1)}} - T_{\beta^{(n)}\beta^{(n+1)}} k_{\beta^{(n+1)}}. \quad (43)$$

Given our definition in Eq. 8, and the fact that β is α with a 1 added, we can rearrange this to give

$$k_{\alpha^{(n)}} - k_{\beta^{(n)}} = T_{\alpha^{(n)}\alpha^{(n+1)}} (k_{\alpha^{(n+1)}} - k_{\beta^{(n+1)}}) + \frac{q}{p} k_{\beta^{(n+1)}}. \quad (44)$$

From this we can see that if $k_{\alpha^{(n+1)}} \geq k_{\beta^{(n+1)}}$ then we must have $k_{\alpha^{(n)}} \geq k_{\beta^{(n)}}$. Now, by construction we know that $\alpha^{(n)} = \beta^{(n)} \forall n \geq t$, since this is the point at which

the additional 1 in the memory is removed. In turn this means that $k_{\alpha(n)} = k_{\beta(n)} \forall n \geq t$. Inductively this gives us that

$$k_{\alpha(t-1)} \geq k_{\beta(t-1)}, \dots, k_{\alpha(n+1)} \geq k_{\beta(n+1)}. \quad (45)$$

Thus we have that $k_{\alpha(n)} \geq k_{\beta(n)}$. Hence we have proved that k_{α} is decreased by adding a one at any point in the memory, and, equally, increased by adding a zero at any point in the memory.

The first statement gives us that, since we can not guarantee that $k_4 > 1/y$, we can not guarantee that, for any state α with a single one in any position other than 1, $k_{\alpha} > 1/y$. The second statement then tells us that, since any state α can be generated by taking a state with only a single 1 somewhere, and adding more 1's to it, we can never guarantee that $k_{\alpha} > 1/y$ for any $\alpha \geq 4$.

Because of this we see that for small y we must have $\langle \tau^p \rangle \geq \langle \tau^{\infty} \rangle$, and hence we must have $\langle \tau^p \rangle \geq \langle \tau^0 \rangle$, finally giving us that $\mathfrak{P}^p \geq 1$. However, for larger y this may not be the case.

G. Correlations in the correlated model

By introducing a probability that a link in a DARN(p) network can draw from the memory of another link, and hence creating the CDARN(p) model, we have introduced correlations. The extent of these correlations can be completely characterised analytically. If we have a network with L possible links, each with their own linear index, let us denote the correlations between link ℓ and ℓ' at time lag k as $\langle A_t^{\ell} A_{t-k}^{\ell'} \rangle = \rho_k^{\ell\ell'}$. Following the procedures in [35, 57], we can derive the following Yule-Walker equations

$$\rho_k^{\ell\ell'} = \frac{q}{p} \sum_{a=1}^p \sum_{b=1}^L c^{\ell b} \rho_{k-a}^{b\ell'}, \quad (46)$$

where the elements $c_{\ell b}$ are taken from the coupling matrix assigning the probability of a link ℓ drawing from the memory of link b . This can be written more compactly in terms of the corresponding matrices ρ_k and C as

$$\rho_k = \frac{q}{p} C \sum_{a=1}^p \rho_{k-a}. \quad (47)$$

These equations can be solved given a suitable closure. Following [35], we can re-write this expression for values of $k < p$ as

$$\rho_k = \frac{q}{p} C \left(\sum_{a=1}^{k-1} \rho_a + \sum_{a=1}^{p-k} \rho_a + \rho_0 \right), \quad (48)$$

assuming some currently unknown value for ρ_0 . This equation can be seen to have a constant solution ρ given by the solution to

$$\rho = \frac{q}{p} C ((p-1)\rho + \rho_0) \quad (49)$$

Now we need to find a suitable expression for ρ_0 . We know that, by definition, $\rho_0^{\ell\ell} = 1$. The off diagonal entries however are given by the Yule-Walker equation

$$\rho_0^{\ell\ell'} = \frac{q}{p} \sum_{a=1}^p \sum_{b=1}^L c^{\ell b} \rho_a^{b\ell'}. \quad (50)$$

But, we know that the value of ρ_a must be a constant ρ , and so the off-diagonal elements of ρ_0 will be the same as the off-diagonal elements of

$$\begin{aligned} \bar{\rho}_0 &= \frac{q}{p} \sum_{a=1}^p C \rho, \\ &= q C \rho. \end{aligned} \quad (51)$$

Putting everything together we get the equation

$$\rho^{\ell\ell'} = \frac{q}{p} \left((p-1) \sum_{b=1}^L c^{\ell b} \rho^{b\ell'} + q \sum_{b \neq \ell'}^L \sum_{\ell''=1}^L c^{\ell b} c^{b\ell''} \rho^{\ell''\ell'} + c^{\ell\ell'} \right). \quad (52)$$

This can be rearranged to give

$$\rho^{\ell\ell'} = \frac{q}{p} \left(\sum_{\ell''=1}^L \left((p-1) c^{\ell\ell''} + q \sum_{b \neq \ell'} c^{\ell b} c^{b\ell''} \right) \rho^{\ell''\ell'} + c^{\ell\ell'} \right). \quad (53)$$

This can be further simplified by constructing the tensor Δ as

$$\Delta^{\ell\ell'\ell''} = \frac{q}{p} \left((p-1) c^{\ell\ell''} + q \sum_{b \neq \ell'} c^{\ell b} c^{b\ell''} \right), \quad (54)$$

The system of equations given in Eq. 49 can then be written as

$$\rho^{\ell\ell'} = \sum_{\ell''=1}^L \Delta^{\ell\ell'\ell''} \rho^{\ell''\ell'} + \frac{q}{p} c^{\ell\ell'}. \quad (55)$$

This form is more easily dealt with in numerical applications, as a simple dimensional reduction (flattening) yields a more traditional form for a system of linear equations. Importantly, this solution relies on no properties of the coupling matrix other than stochasticity, which it must have by definition. In special cases, such as those where coupling is uniform or symmetric, we can simplify these equations further by analysing the symmetries that arise in C and Δ .

H. Evolution of the autocorrelation function

We wish to now show that the full extent of the autocorrelations in our model are described by the constant value ρ , given over the first p time steps. We first notice that from Eq. 47 we can obtain the following

$$\begin{aligned} \rho_k - \rho_{k-1} &= \frac{q}{p} C \left(\sum_{t=1}^p \rho_{k-t} - \sum_{t=1}^p \rho_{k-t-1} \right), \\ &= \frac{q}{p} C (\rho_{k-1} - \rho_{k-p-1}), \end{aligned} \quad (56)$$

and hence

$$\rho_k - \left(I_d + \frac{q}{p} C \right) \rho_{k-1} = -\frac{q}{p} C \rho_{k-p-1}. \quad (57)$$

However, we know that for $k \in \{1, \dots, p\}$ the autocorrelation is a constant $\rho_k = \rho$, meaning that for $k \in \{p+1, \dots, 2p+1\}$ Eq. 57 becomes

$$\rho_k - \left(I_d + \frac{q}{p} C \right) \rho_{k-1} = -\frac{q}{p} C \rho. \quad (58)$$

This is now a first order inhomogeneous difference equation with solution

$$\rho_k = \rho - e^{k \log(1 + \frac{q}{p} C)} R, \quad (59)$$

Where R is a constant matrix. By noticing that $\rho_{p+1} = qC\rho$ we obtain the expression

$$R = (1-q)\rho \left(1 + \frac{q}{p} \right)^{-(p+1)}. \quad (60)$$

With this solution we see that the equation governing the next p values of ρ_k is of the form

$$\rho_k - \bar{q}\rho_{k-1} = -A + e^{-\lambda k} B, \quad (61)$$

where \bar{q} , A , B and λ are constant matrices. This equation has a general solution

$$\rho_k = A' - e^{-\lambda k} B'. \quad (62)$$

Moreover, in our specific case we find that $A' = \rho$ and $\lambda = \log\left(1 + \frac{q}{p} C\right)$. This implies that not only is the autocorrelation function for the CDARN(p) process exponentially decreasing for all values of k larger than $p+1$, but also that this decay varies according to a single parameter B' every p time steps. This gives us a full picture of the autocorrelations for a CDARN(p) process.

I. Special case: totally symmetric cross correlation

The simplest case of our correlated DARN(p) model occurs when the coupling matrix C is such that $c^{\ell\ell'} = 1/L$, regardless of the links in question. Here we can immediately notice that our tensor Δ now takes the form

$$\Delta^{\ell\ell'\ell''} = \frac{q}{p} \left((p-1)\frac{1}{L} + q\frac{L-1}{L^2} \right). \quad (63)$$

This is invariant over the three indexes ℓ, ℓ' and ℓ'' , and so $\rho^{\ell\ell'}$ must be invariant over ℓ and ℓ' . Hence all of the lagged correlations have the same value, and we can write $\rho^{\ell\ell'} = \rho$ and $\Delta^{\ell\ell'\ell''} = \Delta$, giving us the following equation:

$$\rho = L\Delta\rho + \frac{q}{Lp}. \quad (64)$$

Solving for ρ gives

$$\rho = \left(Lp \left(\frac{1}{q} - 1 \right) + (1-q)L + q \right)^{-1}. \quad (65)$$

This gives us a full picture of the lagged correlations present in the system. All that remains is to find the time 0 correlations $\rho_0^{\ell\ell'}$ for $\ell \neq \ell'$. We can find $\rho_0^{\ell\ell'}$ when $\ell \neq \ell'$ as follows:

$$\begin{aligned} \rho_0^{\ell\ell'} &= \frac{q}{Lp} \sum_{a=1}^p \sum_{b=1}^L \rho_a^{b\ell'}, \\ &= \frac{q}{Lp} L \sum_{a=1}^p \rho_a, \\ &= q\rho. \end{aligned} \quad (66)$$

Since from the above we know that for $1 \leq a \leq p$ ρ_a is the constant ρ we then know that when $\ell \neq \ell'$ $\rho_0^{\ell\ell'} = q\rho$.

Note first that if $L = 1$ then we recover the ACF function for a DAR(p) process. Also note that as L increases this value must decrease, meaning that for large networks both correlations and autocorrelations are removed, and so memory no longer has any effect on the evolution of the system.

J. Special case: uniform cross correlation

The second special case we will consider is that of uniform cross correlation (UCC), as induced by a symmetric coupling matrix. Specifically this means that we require that C be symmetric, with $c^{\ell\ell} = 1 - c$ for all values of ℓ and some given value of c , and $c^{\ell\ell} = \bar{c}$ for $\ell \neq \ell'$ with $\bar{c} = c/(L-1)$. Going back to the general case in Eq. 55 we notice that these conditions ensure that $\rho^{\ell\ell}$ is invariant of ℓ , and when $\ell \neq \ell'$ $\rho^{\ell\ell'}$ is invariant of ℓ or ℓ' . This means that all of the values of $\rho^{\ell\ell'}$ can be found as the solutions to the two following equations (note that $\ell \neq \ell'$ is assumed here)

$$\begin{aligned} \rho^{\ell\ell} &= \sum_{\ell'' \neq \ell} \Delta^{\ell\ell\ell''} \rho^{\ell''\ell} + \Delta^{\ell\ell\ell} \rho^{\ell\ell} + \frac{q}{p}(1-c), \\ \rho^{\ell\ell'} &= \sum_{\ell'' \neq \ell, \ell'} \Delta^{\ell\ell'\ell''} \rho^{\ell''\ell'} + \Delta^{\ell\ell'\ell} \rho^{\ell\ell'} + \Delta^{\ell\ell'\ell'} \rho^{\ell'\ell'} + \frac{q}{p}\bar{c}. \end{aligned} \quad (67)$$

Hence we need only find the relevant values of Δ to proceed. Given the definition of Δ and c and \bar{c} we can find the following

$$\begin{aligned} \Delta^{\ell\ell\ell} &= \frac{q}{p} ((p-1)(1-c) + q(L-1)\bar{c}^2) = \Delta^1, \\ \Delta^{\ell\ell\ell'} &= \frac{q}{p} ((p-1)\bar{c} + q\bar{c}((1-c) + (L-2)\bar{c})) = \Delta^2, \\ \Delta^{\ell\ell'\ell} &= \frac{q}{p} ((p-1)(1-c) + q((1-c)^2 + (L-2)\bar{c}^2)) = \Delta^3, \\ \Delta^{\ell\ell'\ell'} &= \Delta^{\ell\ell\ell'} = \Delta^2, \\ \Delta^{\ell\ell'\ell''} &= \frac{q}{p} ((p-1)\bar{c} + q\bar{c}(2(1-c) + (L-3)\bar{c})) = \Delta^4. \end{aligned}$$

Noticing that $\Delta^{\ell\ell'}$ and $\Delta^{\ell'\ell''}$ are invariant of ℓ, ℓ' and ℓ'' (down to excluded values) we then obtain the following pair of equations:

$$\begin{aligned}\rho^{\ell\ell} &= (L-1)\Delta^2\rho^{\ell\ell'} + \Delta^1\rho^{\ell\ell} + \frac{q}{p}(1-c), \\ \rho^{\ell\ell'} &= (\Delta^3 + (L-2)\Delta^4)\rho^{\ell\ell'} + \Delta^2\rho^{\ell\ell} + \frac{q}{p}\bar{c}.\end{aligned}\quad (69)$$

This gives us a simple, solvable pair of equations. Note that while the full solution in terms of q, p, c and L is easy to obtain now, we will not write it down here due to its length. To find the time 0 correlations we can use Eq. 51 to obtain

$$\rho_0^{\ell\ell'} = q \left(((1-c) + (L-2)\bar{c})\rho^{\ell\ell'} + \bar{c}\rho^{\ell\ell} \right). \quad (70)$$

Competing the description of the correlations for the UCC model.

K. Uniform cross correlation in the large network limit

The uniform cross correlation (UCC) model for CDARN(p) networks is introduced to “spread” any temporal correlations between links over the entire network. In doing this we want to reduce the influence that any such correlations might have on the diffusion process, while keeping everything else about the model the same. What we now show is that when the backbone of the temporal network has a large number of links then the UCC model is indistinguishable from a DARN(p) model that has been restricted to the same backbone, and hence the temporal correlations between links is completely removed.

Consider a CDARN(p) network A_t with L links, memory strength q , link density y and memory length p and a coupling matrix defined by the UCC model. The conditional probability of a link l occurring at time t , given the past p states of the network can be thought of in terms of contributions from the memory of the link itself, the memory of all other links, and some background contribution. This can hence be written as follows:

$$\text{Prob}(a_t^l | \{A_\tau\}_{\tau=t}^{t-p}) = (1-q)y + q((1-c)\phi_{self} + c\phi_{other}), \quad (71)$$

where ϕ_{self} and ϕ_{other} represent the contributions to the conditional from the past p states of the link l and every other link respectively.

For links to be effectively independent then we require that as $L \rightarrow \infty$, ϕ_{other} tends to a constant, and hence the link l has no memory of the past states of any other link. To show this we study the memory kernels ϕ_{self} and ϕ_{other} directly as:

$$\begin{aligned}\phi_{self} &= \frac{(1-c)}{p} \sum_{k=1}^p a_{t-k}^l, \\ \phi_{other} &= \frac{c}{(L-1)p} \sum_{\ell' \neq \ell} \sum_{k=1}^p a_{t-k}^{\ell'}.\end{aligned}\quad (72)$$

We need only focus on ϕ_{other} . First, let us consider the average value

$$\left\langle a_{t-k}^{\ell'} \right\rangle_{\ell'} = \text{Prob}(a_{t-k}^{\ell'} = 1). \quad (73)$$

The CDARN(p) network is taken to be in a stationary state, and so the symmetry of the links under any relabelling guarantees us that $\text{Prob}(a_{t-k}^{\ell'})$ is the same for each link ℓ' and for each time $t-k$. Hence we can write $\text{Prob}(a_{t-k}^{\ell'}) = \bar{a}$ for some constant \bar{a} . Then we must have, for any of the $L-1$ possible values of ℓ' ,

$$\left\langle a_{t-k}^{\ell'} \right\rangle_{\ell'} = \bar{a}. \quad (74)$$

Now, ϕ_{other} can be re-written as follows:

$$\phi_{other} = \frac{1}{p} \sum_{k=1}^p \frac{1}{L-1} \sum_{\ell' \neq l} a_{t-k}^{\ell'}. \quad (75)$$

Then, by the law of large numbers we can express this in terms of the sample average:

$$\begin{aligned}\phi_{other} &= \frac{1}{p} \sum_{k=1}^p \left\langle a_{t-k}^{\ell'} \right\rangle_{\ell'}, \\ &= \frac{1}{p} \sum_{k=1}^p \bar{a}, \\ &= \bar{a}.\end{aligned}\quad (76)$$

Hence $\phi_{other} \rightarrow \bar{a}$ as $L \rightarrow \infty$. Indeed, we can further see that $\bar{a} = y$. Since there are no terms containing links other than l in ϕ_{self} , then we can conclude that the conditional probability is such that, in the same limit $L \rightarrow \infty$,

$$\text{Prob}(a_t^\ell = 1 | \{A_\tau\}_{\tau=t}^{t-p}) \rightarrow \text{Prob}(a_t^\ell = 1 | \{a_\tau^\ell\}_{\tau=t}^{t-p}), \quad (77)$$

and so any memory of other links is lost. To show that this is equivalent to a DARN(p) network we need only look at the conditional probability of obtaining a link in such a network with memory strength \bar{q} , memory length p , link density \bar{y} and adjacency matrix E_t with entries e_t^ℓ :

$$\text{Prob}(e_t^\ell = 1 | \{E_\tau\}_{\tau=t}^{t-p}) = (1-\bar{q})\bar{y} + \frac{\bar{q}}{p} \sum_{k=1}^p e_{t-k}^\ell. \quad (78)$$

Now, by setting the values of \bar{q} and \bar{y} , in terms of the values q, y and c from the CDARN(p) model, to be

$$\begin{aligned}\bar{q} &= q(1-c), \\ \bar{y} &= y,\end{aligned}\quad (79)$$

we obtain that

$$\text{Prob}(e_t^\ell = 1 | \{E_\tau\}_{\tau=t}^{t-p}) = \text{Prob}(a_t^\ell = 1 | \{A_\tau\}_{\tau=t}^{t-p}). \quad (80)$$

Hence the UCC model is precisely a DARN(p) model in the limit of $L \rightarrow \infty$.

-
- [1] M. C. González, C. A. Hidalgo, and A.-L. Barabási, *Nature* **453**, 779 EP (2008).
- [2] P. Singer, D. Helic, B. Taraghi, and M. Strohmaier, *PLOS ONE* **9**, 1 (2014).
- [3] M. Starnini, A. Baronchelli, and R. Pastor-Satorras, *Physical Review Letters* **110**, 168701 (2013).
- [4] E. Yoneki, D. Greenfield, and J. Crowcroft, in *2009 International Conference on Advances in Social Network Analysis and Mining* (2009) pp. 356–361.
- [5] R. Murcio, A. P. Masucci, E. Arcaute, and M. Batty, *Physical Review E* **92**, 062130 (2015).
- [6] D. Li, B. Fu, Y. Wang, G. Lu, Y. Berezin, H. E. Stanley, and S. Havlin, *Proceedings of the National Academy of Sciences* **112**, 669 (2015).
- [7] P. Mazzarisi, P. Barucca, F. Lillo, and D. Tantari, *European Journal of Operational Research* (2019), 10.1016/j.ejor.2019.07.024.
- [8] M. Valencia, J. Martinerie, S. Dupont, and M. Chavez, *Physical Review E* **77**, 050905 (2008).
- [9] F. D. V. Fallani, V. Latora, L. Astolfi, F. Cincotti, D. Mattia, M. G. Marciari, S. Salinari, A. Colosimo, and F. Babiloni, *Journal of Physics A: Mathematical and Theoretical* **41**, 224014 (2008).
- [10] A. P. Millán, J. Torres, S. Johnson, and J. Marro, *Nature Communications* **9**, 2236 (2018).
- [11] D. R. Chialvo, *Nature Physics* **6**, 744 (2010).
- [12] P. Grindrod and D. J. Higham, *Proceedings of the Royal Society of London A: Mathematical, Physical and Engineering Sciences* **466**, 753 (2010).
- [13] P. Holme and J. Saramäki, *Physics Reports* **519**, 97 (2012), temporal Networks.
- [14] N. Masuda and R. Lambiotte, *A Guide to Temporal Networks* (World Scientific (Europe), 2016).
- [15] L. Gauvin, A. Panisson, and C. Cattuto, *PloS one* **9**, e86028 (2014).
- [16] M. Zanin, L. Lacasa, and M. Cea, *Chaos: An Interdisciplinary Journal of Nonlinear Science* **19**, 023111 (2009).
- [17] V. Nicosia, J. Tang, M. Musolesi, G. Russo, C. Mascolo, and V. Latora, *Chaos: An interdisciplinary journal of nonlinear science* **22**, 023101 (2012).
- [18] T. Weng, J. Zhang, M. Small, R. Zheng, and P. Hui, *Scientific reports* **7**, 41951 (2017).
- [19] T. P. Peixoto and M. Rosvall, *Nature Communications* **8**, 582 (2017).
- [20] A. Buscarino, L. Fortuna, M. Frasca, and V. Latora, *EPL (Europhysics Letters)* **82**, 38002 (2008).
- [21] M. Starnini and R. Pastor-Satorras, *Physical Review E* **89**, 032807 (2014).
- [22] M. Karsai, N. Perra, and A. Vespignani, *Scientific reports* **4**, 4001 (2014).
- [23] L. Alessandretti, K. Sun, A. Baronchelli, and N. Perra, *Physical Review E* **95**, 052318 (2017).
- [24] M. Szell, R. Sinatra, G. Petri, S. Thurner, and V. Latora, *Scientific Reports* **2**, 457 EP (2012).
- [25] R. Lambiotte, M. Rosvall, and I. Scholtes, *Nature Physics* , 1 (2019).
- [26] V. Salnikov, M. T. Schaub, and R. Lambiotte, *Scientific reports* **6**, 23194 (2016).
- [27] J. T. Matamalas, M. De Domenico, and A. Arenas, *Journal of The Royal Society Interface* **13**, 20160203 (2016).
- [28] M. Rosvall, A. V. Esquivel, A. Lancichinetti, J. D. West, and R. Lambiotte, *Nat. Commun.* **5**, 4630 (2014).
- [29] A. Moinet, A. Barrat, and R. Pastor-Satorras, *Physical Review E* **98**, 022303 (2018).
- [30] Y. Zhang, A. Garas, and I. Scholtes, arXiv preprint arXiv:1701.06331 (2017).
- [31] T. Hiraoka and H.-H. Jo, *Scientific Reports* **8**, 15321 (2018).
- [32] A. Sapienza, A. Barrat, C. Cattuto, and L. Gauvin, *Physical Review E* **98**, 012317 (2018).
- [33] I. Z. Kiss, G. Röst, and Z. Vizi, *Physical review letters* **115**, 078701 (2015).
- [34] T. P. Peixoto and L. Gauvin, *Scientific reports* **8**, 15511 (2018).
- [35] O. E. Williams, F. Lillo, and V. Latora, *New Journal of Physics* **21**, 043028 (2019).
- [36] A. Moinet, R. Pastor-Satorras, and A. Barrat, *Physical Review E* **97**, 012313 (2018).
- [37] N. Masuda, K. Klemm, and V. M. Eguíluz, *Physical Review Letters* **111**, 188701 (2013).
- [38] J.-C. Delvenne, R. Lambiotte, and L. E. Rocha, *Nature Communications* **6**, 7366 (2015).
- [39] I. Scholtes, N. Wider, R. Pfitzner, A. Garas, C. J. Tesse, and F. Schweitzer, *Nature Communications* **5**, 5024 (2014).
- [40] X.-X. Zhan, A. Hanjalic, and H. Wang, *Scientific reports* **9**, 6798 (2019).
- [41] H.-H. Jo, J. I. Perotti, K. Kaski, and J. Kertész, *Physical Review E* **92**, 022814 (2015).
- [42] R. Burioni, E. Ubaldi, and A. Vezzani, *Journal of Statistical Mechanics: Theory and Experiment* **2017**, 054001 (2017).
- [43] H. Kim, M. Ha, and H. Jeong, *The European Physical Journal B* **88**, 315 (2015).
- [44] N. Georgiou, I. Z. Kiss, and E. Scalas, *Physical Review E* **92**, 042801 (2015).
- [45] I. Scholtes, in *Proceedings of the 23rd ACM SIGKDD International Conference on Knowledge Discovery and Data Mining* (ACM, 2017) pp. 1037–1046.
- [46] R. Lambiotte, V. Salnikov, and M. Rosvall, *Journal of Complex Networks* **3**, 177 (2015).
- [47] C. L. Vestergaard, M. Génois, and A. Barrat, *Physical Review E* **90**, 042805 (2014).
- [48] E. R. Colman and D. Vukadinović Greetham, *Physical Review E* **92**, 012817 (2015).
- [49] D. J. Watts and P. S. Dodds, *Journal of consumer research* **34**, 441 (2007).
- [50] F. Schweitzer, *Brownian agents and active particles: collective dynamics in the natural and social sciences* (Springer, 2007).
- [51] T. Di Matteo, T. Aste, and S. Hyde, arXiv preprint cond-mat/0310544 (2003).
- [52] A. Arenas, A. Díaz-Guilera, J. Kurths, Y. Moreno, and C. Zhou, *Physics Reports* **469**, 93 (2008).
- [53] S. Boccaletti, V. Latora, Y. Moreno, M. Chavez, and D.-U. Hwang, *Physics reports* **424**, 175 (2006).
- [54] M. Newman, *Networks: an introduction* (Oxford university press, 2010).
- [55] P. Van Mieghem and R. van de Bovenkamp, *Physical Review Letters* **110**, 108701 (2013).
- [56] W. Min and L. Wynter, *Transportation Research Part C: Emerging Technologies* **19**, 606 (2011).

- [57] P. A. Jacobs and P. A. Lewis, *Discrete Time Series Generated by Mixtures. III. Autoregressive Processes (DAR(p))*, Tech. Rep. (NAVAL POSTGRADUATE SCHOOL MONTEREY CALIF, 1978).
- [58] J. D. Hamilton, *Economic Theory*. II, Princeton University Press, USA , 625 (1995).
- [59] J. Runge, V. Petoukhov, J. F. Donges, J. Hlinka, N. Jaccay, M. Vejmelka, D. Hartman, N. Marwan, M. Paluš, and J. Kurths, *Nature Communications* **6**, 8502 EP (2015).
- [60] B. Bollobás, *Random graphs*, 73 (Cambridge university press, 2001).
- [61] “Us airports network dataset – KONECT,” (2016).
- [62] R. Michalski, S. Palus, and P. Kazienko, in *Lecture Notes in Business Information Processing*, Vol. 87 (Springer Berlin Heidelberg, 2011) pp. 197–206.
- [63] T. for London, “Rolling origin and destination survey (rods),”.
- [64] E. Cinlar, *Introduction to Stochastic Processes*, Dover Books on Mathematics Series (Dover Publications, Incorporated, 2013).
- [65] C. Ballester and M. Vorsatz, *Review of Economics and Statistics* **96**, 383 (2014).
- [66] I. L. MacDonald and W. Zucchini, *Hidden Markov and other models for discrete-valued time series*, Vol. 110 (CRC Press, 1997).